HHS Public Access

Author manuscript

Calcif Tissue Int. Author manuscript; available in PMC 2021 November 27.

Published in final edited form as:

Calcif Tissue Int. 2016 February ; 98(2): 172–185. doi:10.1007/s00223-015-0076-4.

Sex-linked Skeletal Phenotype of Lysyl Oxidase Like-1 Mutant Mice

Loai Alsofi[1,2,‖], **Eileen Daley**[1,‖], **Ian Hornstra**[3], **Elise F. Morgan**[4], **Zachary D. Mason**[4], **Jesus F. Acevedo**[5], **R. Ann Word**[5], **Louis C. Gerstenfeld**[6], **Philip C. Trackman**[1,*]

[1]Boston University Henry M. Goldman School of Dental Medicine, Department of Molecular and Cell Biology, Boston, MA 02118

[2]King Abdulaziz University, Department of Endodontics, Faculty of Dentistry, King Abdulaziz University, Jeddah, Saudi Arabia

[3]Washington University School of Medicine, Division of Dermatology, St. Louis, MO

[4]Boston University, Department of Mechanical Engineering, 110 Cummington Mall, Boston, MA 02215

[5]University of Texas Southwestern Medical Center, Department of Obstetrics and Gynecology, Dallas, TX 75390

[6]Boston University School of Medicine, Department of Orthopaedic Surgery, Boston, MA 02118

Abstract

Lysyl oxidases are required for collagen and elastin cross-linking and extracellular matrix maturation including in bone. The lysyl oxidase family consists of lysyl oxidase (LOX) and 4 isoforms (LOXL1–4). Here we investigate whether deletion of LOXL1, which has been linked primarily to elastin maturation, leads to skeletal abnormalities. Left femurs (n=8), L5 vertebrae (n=8) and tibiae (n=8) were analyzed by micro-computed tomography (μCT) in 13-week old wild type (WT) and *LOXL1*−/− male and female mice. Right femurs (n=8) were subjected to immunohistochemistry for LOXL1, and histochemical/histology analyses of osteoclasts and growth plates. Sera from all mice were analyzed for bone turnover markers. Results indicate strong expression of LOXL1 in wild type growth plates in femurs. Significant deterioration of trabecular bone structure in long bones and vertebrae from female was observed in not from male, mutant mice compared with WT. Decreases in BV/TV, Conn.D, and trabecular thickness and number in the femoral distal metaphysis were observed in female, but not male, mutant mice. Trabecular spacing was increased significantly in femurs of female mutant mice. Findings were similar in trabeculae of L5 vertebrae from female mutant mice. The number of TRAP positive osteoclasts at the trabecular bone surface was increased in female mutant mice compared with WT females, consistent with increased serum RANKL and decreased OPG levels. Analysis of bone turnover markers confirmed increased bone resorption as indicated by significantly elevated CTX-1 in the

*Corresponding author: Philip C. Trackman, Boston University, Henry M. Goldman School of Dental Medicine, Department of Molecular and Cell Biology, 700 Albany Street; W-201, Boston, MA 02118, Telephone: (617) 638-4076, trackman@bu.edu.

‖These authors contributed equally to this study.

Conflicts of Interest

All authors declare no conflicts of interest.

serum of female *LOXL1−/−* mice compared to their wild-type counterparts, as well as decreased bone formation as measured by decreased serum levels of PINP. Picrosirius red staining revealed a loss of heterogeneity in collagen organization in female *LOXL1−/−* mice only, with little to no yellow and orange birefringence. Organization was also impaired in chondrocyte columns in both female and male *LOXL1−/−* mice, but to a greater extent in females. Data indicate that *LOXL1−/−* mutant mice develop appendicular and axial skeletal phenotypes characterized by decreased bone volume fraction and compromised trabecular microstructure, predominantly in females.

Keywords

lysyl oxidases; micro-computed tomography; collagen; cross-link; phenotype; bone histomorphometry; osteoclasts; bone μCT; genetic animal model; cytokines

Introduction

The lysyl oxidase sub-family of copper dependent amine oxidase enzymes catalyzes the oxidative deamination of peptidyl-lysine or hydroxylysine residues to create reactive aldehydes in the biosynthesis of collagens and elastin. These modifications are required for subsequent spontaneous cross-link formation and function of these connective tissue proteins [1]. The five members of the lysyl oxidase family are respectively encoded by different genes and are lysyl oxidase (*LOX*) and lysyl oxidase like 1–4 (*LOXL1–4*). These proteins have more recently been implicated in a number of novel and diverse biological roles that extend from promoting proliferation during cell development to shifts from normal to malignant phenotypes in cancer [2–4]. The C-terminal domains of LOX and its family members have sequence and structural similarity, and contain the active site of the enzymes. LOX and LOXL1 are closely related in structure, both containing a pro-region that is post-translationally processed, and both lack the scavenger receptor cysteine rich domain present in LOXL2-LOXL4 [5]. LOX is synthesized as a 50 kDa pro-enzyme and is secreted. Proteolytic processing by extracellular pro-collagen C-proteinases releases the ~30 kDa mature lysyl oxidase enzyme and the ~18 kDa pro-peptide (LOX-PP) [6–8]. LOXL1 is similarly processed by pro-collagen C- proteinases to an active 33 kDa enzyme [9]. LOXL1 function has been linked primarily to elastin tissue maturation [10]. The reactive aldehydes created by the oxidative deamination catalyzed by lysyl oxidase and its isoforms are critical in forming intra- and inter-molecular cross-links needed to stabilize collagens and elastin [11, 12]. These cross-links are required for the integrity of the extracellular matrix in connective tissues, including bone and cartilage in which the predominant proteins are type II and type I collagen, respectively. Defects in LOX activity result in abnormal mineralized tissue [13]; however a role for LOXL1 in bone formation has not been reported.

Lysyl oxidase inhibition by BAPN or copper depletion results in lathyrism, which is characterized by a variety of connective tissue abnormalities [14]. *Lox−/−* mice exhibit perinatal death and have connective tissue abnormalities in the cardiovascular and respiratory systems similar to lathyrism [15, 16], and abnormalities have been observed in cultured calvaria osteoblasts from *LOX−/−* embryos [17]. Osteoporosis is a heterogeneous group of abnormal processes characterized by the net loss of bone and increased

susceptibility to fracture. By histomorphometric analysis, there is a decrease in the number and size of trabecula in cancellous bone, as well as increases in trabecular perforations and decreases in trabecular connectivity [18]. Estrogen deficiency is a significant cause of accelerated bone loss and is known to affect circulating levels of specific cytokines whose modulation results in enhanced bone resorption by increasing the recruitment, differentiation, and activation of osteoclast cells [19]. Furthermore, estrogen has various influences on connective tissue metabolism [20]. Diabetic osteopenia is also characterized by defective connective tissue, specifically a decrease in biosynthetic lysyl oxidase dependent cross-links per unit of collagen in normal bone tissue [21]. The aim of the present study was to investigate the skeletal phenotype in mice genetically deficient in the LOXL1 isoform, and determine whether any phenotype found could resemble bone pathologies such as those seen in osteoporosis or diabetic osteopenia. Since *LOX*−/− mice are neonatal lethal, the LOXL1 isoform was chosen for the current study because its structure is the most similar of the four other isoforms to LOX, and because LOX and LOXL1 are expressed by osteoblasts [17, 22]. The present study reveals sex-specific deficiencies in trabecular structure with evidence for increased osteoclast activity in *LOXL1*−/− mice compared to wild-type littermate control mice. The sex-specific abnormalities in trabecular structure and cytokine profiles of the *LOXL1*−/− mice are of great interest and may suggest hormonal regulation of LOXL1 that could be of possible functional significance in sex-specific bone developmental programs and pathologies.

Materials and Methods

Mouse Tissues

LOXL1−/− mice were generated in accordance with a previously published strategy employed for generating *LOX* null mice [15]. The ATG codon of *LOXL1* and surrounding bases of a BAC clone containing *LOXL1* were converted to a *NotI* restriction sites by site-directed mutagenesis (QuikChange mutagenesis, Stratagene, La Jolla, CA). A *NotI* fragment of the modified gene including the PGK-Neo cassette was cloned into the *NotI* site of the mutagenized ATG initiation codon of the *LoxL1* gene construct. This construct deletes the ATG initiation codon and replaces it with the PGK-Neo cassette in the opposite transcriptional orientation. Correctly targeted RW4 embryonic stem cells (129/SvJ), carrying this mutation, were injected into C57BL/6 blastocysts and chimeric mice were produced. This mutation was transmitted into the germline and mice homozygous for this mutation (*LOXL1*−/−) were generated in a mixed 129/SvJ × C57BL/6 background. Mice were identified as heterozygous or homozygous with respect to the targeted allele by PCR of tail tip DNA using nested primers (wild-type: 5’ TTGTTCTCCCACTGGATCAGCTGCC 3’; mutant: 5’ TACCGGTGGATGTGGAATGTGTGCGA 3’; common: 5’ TGGGAAGAGAAGCACGCACCGAG 3’). *LOXL1*−/− mice (backcrossed into the C57BL/6 background for more than 7 generations) were bred at University of Texas Southwestern Medical Center. All tissues were harvested under the same specified conditions from knockout and wild type littermate controls at 13 weeks of age, and all procedures were approved by the respective IACUC committees at both Boston University and University of Texas Southwestern Medical Center. After sacrifice, the left femur, left tibiae, and spines were dissected and wrapped in PBS-soaked paper to be used for

subsequent micro- computed tomography (μ-CT) analyses. The right femurs were fixed in 4% paraformaldehyde and then processed for histological staining and histochemical tartrate resistant alkaline phosphatase (TRAP) analysis at Boston University. This processing was performed at the same time for the mutant and wild type mice.

LOXL1 Immunohistochemistry

The right femur from each animal was fixed in cold 4% paraformaldehyde. Decalcification was performed by dialysis in 14% EDTA (American Bioanalytical, Natick, MA) for three weeks. The bones were then embedded longitudinally in paraffin with the intercondylar notch at the distal end facing upward. Specimens were sectioned at 7 microns and prepared for immunohistochemistry [23]. The primary antibody against LOXL1 was obtained from Abbiotec, catalogue #252215, and was generated against a unique human LOXL1-specific sequence conserved in mice. Sections were visualized using a Zeiss Axio Observer Z1 (Carl Zeiss Microscopy, Jena, Germany), and images captured using ZEN pro software (Carl Zeiss Microscopy, Jena, Germany).

Micro-Computed Tomography and Image Analysis

All μCT analyses of femurs, L5 vertebrae, and tibiae were carried out at the μCT Imaging Core Facility at Boston University using a Scanco Medical μCT40 Scanning instrument (Brütisellen, Switzerland). The power, current, and integration time used for all scans were 70 kVp, 113 μA, and 200 msec respectively. The femurs, spines, and tibiae were all scanned at a resolution of 12 microns/voxel. The software used for the subsequent contouring and analysis was developed by Scanco Medical. Regions selected for trabecular analysis were the trabecular compartments of the distal metaphysis of the femur, the center of the vertebral body of the L5 vertebrae, and the proximal tibial plateau of the tibia. For cortical analysis, the mid diaphysis of the femur, the cortical shell (cortical compartment) of the vertebrae, and the mid diaphysis of the tibia were used for analysis [24]. To determine the trabecular region of interest of the femurs and tibiae, the location of the growth plate was determined and the regions which were 60 microns removed from the end of the growth plate and which extended 1200 microns proximal and distal of the growth plate were respectively analyzed. The entire lengths of the vertebrae were evaluated, comprising a total length of ~3600 microns. Gaussian filtering (sigma= 0.8, support=1) was used for partial background noise suppression. The threshold was set at a 16-bit gray value of 9830 and this global threshold was applied to all of the samples [25]. For contouring the perimeter of the trabecular region, each transverse 2-D tomogram of the vertebra was manually traced to designate the cortical shell and trabecular regions. For separating the cortical and trabecular regions of the femurs and tibiae, an automated method within the system software was used [26]. Trabecular and cortical analyses were performed and reported as described [27].

Osteoclast Density in the Distal Metaphysis

The right femur from each animal was fixed in cold 4% paraformaldehyde, decalcified by dialysis in 14% EDTA (American Bioanalytical, Natick, MA) for three weeks, sectioned and then stained for TRAP activity. The area analyzed was from the bottom of the growth plate extending 2 mm toward the opposite end of the long bone. All osteoclasts were counted in this area, excluding osteoclasts in the cortical shell. Osteoclasts were identified

as TRAP positive, multinucleated cells associated with the bone surface. Other identifiers included size, (25–50 μM in diameter), and association with a resorption pit. Overlapping images were taken on an Olympus FSX100 and analyzed using FSX-BSW v02.02 software (Olympus America Inc., Center Valley, PA) which created a composite picture of the individual low magnification images (100X) taken of the area, as well as higher resolution images (200X). The number of osteoclasts was normalized to millimeter of bone surface of the trabecular contour drawn using Image J software.

Osteoblast Density in the Distal Metaphysis

Osteoblasts were counted using hematoxylin and eosin stained central sections, to better visualize nuclei. Three central sections were chosen for each animal (n=8, total of 24 sections), from composite pictures as described above. Osteoblasts were identified by morphological criteria: cuboidal cells attached to the bone occurring in clusters, having an asymmetrically positioned nucleus, and stained light purple. The number of osteoblasts was normalized to millimeter of bone surface of the trabecular contour drawn using Image J software.

Growth Plate Analysis

The chondrocyte density in the growth plate was calculated by counting the number of cells in each composite image and dividing by the total growth plate area as calculated by Image J software determined from hematoxylin and eosin stained sections. The average number of column forming chondrocytes was calculated by counting the number of cells per column in 5 separate columns and averaging them. The average height of the growth plate was calculated by measuring the height at five different regions across the plate.

Analysis of Collagen Organization

Collagen organization was analyzed using picrosirius red stained central sections as described [28]. Images were visualized using an Olympus IX70 microscope with and without polarizing filters engaged (Olympus Inc., Tokyo, Japan) and captured using Pictureframe software. The area analyzed for each image started at the center of the growth plate and extended ~ 2 mm to the right. Images were analyzed for yellow, orange, and red birefringence.

Serum Immunoassays

Serum from wild-type and mutant mice were tested for relative quantities of the following cytokines: IL-6, TNF-α, osteocalcin (OCN), osteoprotegerin (OPG), and Receptor Activator of Nuclear Factor Kappa-B Ligand (RANKL) via immunoassay using the Milliplex system (EMD Millipore, Billerica MA) according to the manufacturer's instructions. This system utilizes mouse antibody-immobilized beads magnetized to a plate block. Serum samples were diluted 1:2 with assay buffer for all of the protein markers except osteocalcin, which was diluted 1:20. Three separate assays were done, one using 3 antibody immobilized beads consisting of Il-6, OPG, and TNF-α, and two other assays were run on OCN and RANKL single immobilized beads. The plates were read using a Luminex Magpix platform (Luminex, Austin, TX) to identify the fluorescence of the secondary antibody/streptavidin

reporter. Standard curves were generated using standards with known concentrations for all the analytes run. MFIs (median fluorescent intensity) were generated and used to determine the concentration of each analyte. Serum was also analyzed for bone turnover markers procollagen type I N-terminal peptide (PINP) and cross-linked C-telopeptide of type I collagen (CTX-1) using ELISA assays according to the manufacturer (MyBiosource, San Diego, CA, Cat # MBS736256 and Cat# MBS2014019).

Statistical Analysis

For all analyses performed statistics were done by comparison of each mutant to wild type of the corresponding sex by a one way ANOVA. Tukey's post hoc tests were then performed if differences between groups were significant. A p-value of <0.01 was considered to be statistically significant.

Results

Sex-Specific Effects of LOXL1−/− on Trabecular Bone Parameters

LOXL1 was ablated from the mice homozygous for the mutated allele at the DNA (Figure 1) and protein levels were assessed by immunohistochemistry with an antibody specific for the unique N-terminus of LOXL1 (Figure 2). This was indicated by the presence of chondrocyte and extracellular matrix-associated LOXL1 staining in the growth plates of sections made from wild type mice, and the absence of staining in the *LOXL1−/−* male and female femur sections, and all IgG isotype control stained serial sections (Figure 2). No staining was observed in osteoblasts or in cortical bone in any samples suggesting that LOXL1 long bone expression occurs primarily in chondrocytes in 13 week old mice. Knockout mice were viable and grossly normal. Comparisons of weight and femur length indicate that mutant and wild-type controls were similar in size (Table 1). Three dimensional reconstructions of the μCT scans of the distal metaphysis of the femur and the L5 vertebrae show clear abnormalities in trabecular architecture in *LOXL1−/−* female mice relative to wild-type littermates, (Figure 3A–D and 3E–H, respectively). Full-length bone scans of the femur corroborate these results and further indicate that femur length is unaltered in spite of trabecular abnormalities (Figure 3I–L). This effect was also seen in the tibial plateau in *LOXL1−/−* mice (data not shown). These images show that these abnormalities are exclusively seen in *LOXL1−/−* females, while the *LOXL1−/−* males resemble their wild-type counterparts. This is supported by quantitative analyses computed from the μCT scans (Figure 4).

BV was significantly lower in the female, but not in the male, *LOXL1*−/− mice as compared to their wild-type counterparts, whereas total volume was similar for both female and male mutant phenotypes compared to wild-type (Figure 4A and 4B, respectively). This is reflected in significant decreases in BV/TV ratios in *LOXL1−/−* females compared to WT females (p-value < .001) (Figure 4C). In the trabeculae, connectivity density (Conn.D, Figure 3D), trabecular number (Tb.N, Figure 3E) were decreased, trabecular spacing was increased (Tb.Sp, Figure 3F), and trabecular thickness (Tb.Th, Figure 3G) was decreased significantly in *LOXL1−/−* females (p-value <.01). Interestingly, these changes in trabeculae were not observed in *LOXL1−/−* males. Hence, all μCT trabecular parameters tested were

significantly affected in female, but not male, *LOXL1−/−* mice. In contrast, cortical bone parameters were not significantly altered in either female or male *LOXL1−/−* femurs relative to respective wild-type controls (Table 2).

To corroborate results observed in the distal metaphysis of the femur, trabeculae of the L5 vertebrae were analyzed using the same parameters employed for the femurs. The L5 vertebrae also showed significantly low trabecular bone parameters that were sex-specific, compared to their wild-type controls. Specifically, bone volume was significantly low in *LOXL1−/−* females while total volume remained the same across all four genotypes (BV, Figure 5A and 5B). The results, therefore, reflect significant decreases in the BV/TV ratios in trabeculae of *LOXL1−/−* females compared with WT (p-value <0.001) (Figure5C). There were no such effects observed in *LOXL1−/−* males. Further, connective density (Conn.D, Figure 4D), trabecular number (Tb.N, Figure 4E), and trabecular thickness (Tb.Th, Figure 4F) were decreased in *LOXL1−/−* females, but not *LOXL1−/−* males ($p < 0.01$). There were no significant differences in trabecular spacing nor in the cortical parameters of the cortical shell of the L5 vertebrae in any of the mice (Table 2). Together, these results indicate a defect in the trabecular bone architecture of female *LOXL1*−/− mice, which was not observed in cortical bone. Quantitative analyses were also performed on the trabecular bone of the tibiae and showed the same sex-specific abnormalities in all of the μCT parameters tested (data not shown).

Histological Analysis of Bone Resorption and Formation

To determine if increased bone resorption contributed to defective trabecular patterns in *LOXL1−/−* mice, bones were stained for TRAP activity. Representative images clearly show a high concentration of TRAP stain (Figure 6, panel D) and TRAP positive osteoclasts (Figure 6, panel E) in the *LOXL1−/−* females. The number of osteoclasts was next quantified by counting TRAP positive, multinucleated cells. The number of osteoclasts per millimeter of bone area was increased dramatically in *LOXL1−/−* females ($p< 0.0001$, Figure 7A). These results indicate increased resorptive activity in *LOXL1−/−* female mice, which also corresponds to a significant decrease in total bone area in *LOXL1−/−* females determined with Image J software (data not shown). There was no statistically significant increase in TRAP positive cells seen in *LOXL1*−/− males (Figure 7A).

The number osteoblasts per millimeter of bone surface was quantified by counting cuboidal, light purple, clustered cells with an asymmetric nucleus associated with the bone surface in hematoxylin and eosin stained central sections. There were no significant differences between any of the genotypes (Figure 7B). Therefore the increase in bone resorption as indicated by increased osteoclast number is not accompanied by an increase in bone formation as quantified by osteoblast number. If bone formation were to increase with bone resorption, total bone turnover would remain the same. Instead this cytometric analysis points to a cellular uncoupling of bone turnover processes favoring increased resorption as measured by the ratio of osteoclasts to bone-generating osteoblasts (Figure 7C), consistent with the bone deficits evaluated by micro-CT.

Histological Analysis of Cartilage Growth Plates

Representative images of growth plates shown in Figure 8 indicate that columns lack a normal organization in all knockout mice, although the effects were more pronounced in the knockout female mice (Figure 8, panel D). Quantitative analyses of the growth plates revealed significantly lower numbers of chondrocytes per column in both *LOXL1−/−* females and males in comparison to their wild-type counterparts ($p < 0.0001$) (Figure 8E). The average growth plate height and chondrocyte density were not significantly affected in mutant mice however (data not shown), consistent with very similar femur lengths in mutant mice compared to wild-type mice (Table 1).

Histochemical Analysis of Collagen using Picrosirius Red

To examine whether the structural changes observed in the trabeculae and growth plate disorganization are accompanied by changes in the organization of the collagen fibers, picrosirius red staining was performed [28]. The slides were then viewed under both non-polarized light and polarized light to examine collagen birefringence colors which are enhanced under polarized light by sirius red dye. Fibrillar collagens are normally stained red with variations in color corresponding to alignment: yellow and orange fibers are indicative of larger, thick collagen fibers, while green fibers are indicative of thinner collagen fibers. Data in Figure 9 show that while the wild type control mice and *LOXL1−/−* male mice showed a normal mixed birefringence of red, yellow and orange fibers, as well as some green indicative of a higher ordered structure of type I and type II collagen, *LOXL1−/−* female mice showed predominately red birefringence, with very little of the other birefringence colors represented.

Analysis of Bone Biomarkers in Serum

Serum was taken from all mice and analyzed for selected metabolic bone markers using the Milliplex immunoassay system. Two biomarkers showed significant differences in *LOXL1−/−* females only. There was a significant increase in receptor activator of nuclear factor kappa-B ligand (RANKL), a ligand that binds to its corresponding receptor RANK on osteoclast progenitor cells and induces osteoclast differentiation ($p\text{-value} < 0.01$). To exacerbate this effect, there was also a significant decrease in osteoprotegerin (OPG), the soluble decoy receptor for RANKL (Figure 10) ($p<0.01$) resulting in an increase in the RANKL/OPG ratio. Interestingly, there were no significant differences seen in *LOXL−/−* males compared to their wild-type counterparts. There were no significant differences in interleukin-6, TNF-α, or osteocalcin concentration between the groups (Figure 10). These results are generally consistent with the μCT and histological characterizations summarized above and indicate that there is sex-specific dysregulation occurring that drives the observed phenotype, though the lack of significant change in IL-6 and TNF-α was not expected.

To further extend the histomorphometric data showing evidence for increased bone resorption, serum was analyzed for bone turnover markers procollagen type I N-terminal propeptide (PINP) which is a sensitive marker for bone formation, and C-terminal telopeptide (CTX-1) which is a cross-linked peptide of type I collagen and the most specific marker for bone resorption [29]. Results indicate not only a significant increase in CTX-1 in female *LOXL1−/−* mice compared to their wild-type counterparts (Figure 11A, $p < 0.05$),

which validates the increased number of osteoclasts seen in these mice, but also a significant decrease in PINP (Figure 11B, $p < 0.01$), indicating an actual decrease in bone formation in female *LOXL1−/−* mice compared to their wild-type counterparts. No such difference was observed in male *LOXL1−/−* mice.

Discussion

Results presented here indicate for the first time that LOXL1 is important for a normal trabecular bone phenotype, particularly in females. Serum analyses for pro-collagen type I N-terminal propeptide (PINP) and C-terminal telopeptide for collagen type I (CTX-1) show not only an increase in CTX-1 marker for bone resorption in female *LOXL1−/−* mice, but also a decrease in PINP marker for bone formation. Differences in growth plate organization were evident in both *LOXL1−/−* females and males, although this effect was much more pronounced in females. The combination of the sex-specific defects in trabecular bone structure and an altered OPG/RANKL cytokine ratio bone suggest an osteoporotic-like condition in the *LOXL1−/−* female mouse bones that may be generally relevant to osteopenia. For example, studies in humans and animals support that osteopenic diabetic bones contain lower levels of lysyl oxidase family-dependent cross-links and higher levels of advanced glycation endproducts (AGEs), as recently reviewed [21].

It is of interest that in 13 week-old mice, LOXL1 expression was observed almost exclusively in and around chondrocytes and in the growth plate extracellular matrix in femurs. We previously reported the expression patterns of all five LOX isoforms in fracture healing and identified a temporal expression pattern which implied high expression particularly in chondrocytes. LOXL2 knockdown studies in the ATDC5 chondrocyte cell line identified a critical role for LOXL2 expression in chondrocyte differentiation [30]. LOXL1- LOXL4 were all up-regulated during the chondrogenic phase of bone healing, but studies in ATDC5 cells indicated that LOXL1 expression as a function of differentiation was constitutive [30]. Here, data in Figure 8 suggest that LOXL1 is critical for chondrocyte growth plate organization in both sexes, with greater effect and consequences on trabecular bone structure in female mice. Taken together, data suggest that while LOXL2 is required for chondrocyte differentiation, LOXL1 contributes to chondrocyte organization with apparent secondary effects on trabecular bone structure. LOXL2 null mice have recently been reported to be perinatal lethal with 50% penetrance, though no sex-correlations for penetrance or bone characterization was presented [31].

There are differences in the severity of the trabecular defects, suggesting that LOXL1 deficiency may affect long bones and vertebrae differently. For example, trabecular defects in the femur were overall more severe than in the vertebrae, with the vertebrae exhibiting no defects in trabecular spacing. Connectivity density was ~50% lower in the femur relative to the vertebrae. Tibiae more closely resembled the femurs in severity (data not shown). In a typical osteoporosis model, the more profound trabecular bone deterioration is observed in the vertebrae, which have trabeculation through the entire length of the vertebral body and is the most common site of fracture [32]. Our findings using LOXL1 null animals suggest that (i) LOXL1 plays crucial roles in bone remodeling that preferentially affect one site more severely than another, and (ii) absence of LOXL1 results in bone pattern defects that are not

typical of osteoporosis. This finding may be related to the possibility that LOXL1 is a major product of chondrocytes, and a relatively minor product of osteoblasts suggested by data in Figure 1.

The LOXL1 isoform has been thought to be most important in elastin biosynthesis [33], whereas direct evidence for a role for LOXL1 in skeletal structure has not been previously reported. The trabecular defects combined with the cytokine profiles reported here in the female *LOXL1−/−* mice suggest cross-talk between expression of lysyl oxidase isoforms and female hormonal regulation or activity. Estrogen increases the activity of LOX in vivo in aging mice that undergo estrogen therapy, and this leads to the acceleration of the maturation of collagen and elastin in the extracellular matrix [20]. Loss of estrogen in post-menopausal women is a main physiological cause of bone loss and subsequent osteoporosis in these women, leading to an increase in fracture [34]. The effects of estrogen loss on the trabecular bones of mice have also been demonstrated [35]. Estrogen exerts its anti-resorptive effects in bone by stimulating the expression of OPG in osteoblasts [36], resulting in the sequestration of RANKL from its receptor RANK on osteoclasts [37]. Immunoassays performed here showed a significant decrease in OPG and a significant increase in RANKL in all female *LOXL1−/−* mice tested, but not in male *LOXL1−/−* mice. This dysregulation tips the scales in favor of increased bone resorption. However, because all mice were cycling and fertile, it is likely that estrogen production from the ovary was similar among WT and *LOXL1−/−* females. Thus, low estrogen levels in *LOXL1−/−* female mice are not likely to have occurred or to have driven the phenotypic sex-specific effects observed here. We speculate that the loss of LOXL1 in some way either interferes with female hormone responses, or that the higher level of androgens in males may induce high levels of LOX or other lysyl oxidase isoforms in bone and compensate for constitutive low levels of LOXL1 in female bones [38]. Further investigation into the sex-specific developmental and hormonal regulation of lysyl oxidase family members in bone is now of considerable interest.

Evidence for increased bone resorption in female knockout bones was further supported by histological analyses including osteoclast and osteoblast number per bone surface [39]. To further support the cytometric analysis and provide a serum read-out for bone turnover, PINP and CTX-1 serum levels were analyzed [40]. It was especially important to examine CTX-1 since this peptide is the portion of type I collagen cleaved by osteoclasts during bone resorption [41]. CTX-1 serum levels were significantly elevated in female *LOXL1−/−* mice compared to their wild-type counterparts, confirming the increase in osteoclast number is accompanied by an increase in osteoclast resorptive activity. Interestingly, PINP levels, a marker of bone formation [29, 42], were decreased in *LOXL1−/−* female mice compared to their wild-type counterparts, suggesting impaired bone formation. Taken together data indicate that dysregulation in the process of bone remodeling female mice in the absence of LOXL1.

Given the role of LOXL1 in fibrillogenesis, and the structural and organization defects seen in the bone and growth plate, it was important to examine the properties of the collagen fibrils directly. Analyses of picosirus red stained sections of growth plates revealed that *LOXL1−/−* female mice have a more homogenous overall birefringence while the other three experimental groups had more normal mixed birefringence profiles. Collagen fiber

structure correlates with the strength of connective tissue, and lysyl oxidases are critical for normal collagen structure. [43, 44]. A multimodal diameter distribution provides connective tissues with the ability to resist different types of mechanical stress, and the structure and organization of collagen fibrils controls hydroxyapatite crystal growth [45]. Therefore the observed loss of heterogeneity in the collagen network of *LOXL1−/−* female mice may have implications in the mineralization of the collagen, leading to the loss of structural integrity observed in these mice.

A trabecular phenotype was observed in LOXL1 null mice, but no significant cortical bone abnormalities were identified by μCT analyses. We speculate that LOXL1 may be most important in bone remodeling rather than bone formation. The phenotype would therefore be more apparent in relatively young 13 week old mice in the trabecular structure which is more dynamic than the cortical bone. Analysis of expression and localization of LOXL1 in bone in developing and aging male and female mice could be informative in this context, and may uncover a period in which LOXL1 is expressed not only by chondrocytes, but also by osteoblasts. LOXL1 expression has been previously detected in MC3T3-E1 cells in vitro [22].

Both *Loxl1−/−* female and male mice have more severely impaired organization of chondrocytes within the distal femur growth plates compared to wild type, suggesting that LOXL1 influences growth plate development independent of sex. However body weights and femur lengths were unaffected in both *LOXL1−/−* female and male mice. Decreased bone growth characteristic of many chondrodysplasias results primarily from defects in chondrocyte proliferation and apoptosis in the proliferative zone of the growth plate [46, 47]. Notably, overall chondrocyte density and growth plate height were the same in the *LOXL1−/−* mice as in their wild-type counterparts; while chondrocyte organization was not normal.

We have reported that LOXL2 is critically required for chondrocyte differentiation in a fracture healing model for endochondral bone development [30], and additional reports indicate that LOX influences cell differentiation independent of its role in collagen cross-linking [2, 48–52]. It is now clear that the lysyl oxidase family is multifunctional and may affect cell signaling directly [52–55]. However, data presented here could also suggest that LOXL1 is somehow regulated by sex hormones such as estrogen or testosterone, and defective collagen resulting from the absence of LOXL1 could trigger the production or release of factors that stimulate osteoclast formation and activity to a greater degree in females than in males due to sex-dependent developmental differences. For example, defective collagen itself can cause an inflammatory response which may be higher in females, leading to a subsequent increase in the production or release of RANKL by osteoblasts and immune cells, resulting in increased osteoclast activity [56]. Further mechanistic studies will be needed to elucidate the mechanisms by which loss of LOXL1 can lead to observed bone phenotypes.

Acknowledgements

This study was supported by DE14066 (PCT), and AG028048 (RAW).

References

1. Csiszar K (2001) Lysyl oxidases: a novel multifunctional amine oxidase family. Progress in nucleic acid research and molecular biology 70:1–32 [PubMed: 11642359]
2. Khosravi R, Sodek KL, Xu WP, Bais MV, Saxena D, Faibish M, Trackman PC (2014) A novel function for lysyl oxidase in pluripotent mesenchymal cell proliferation and relevance to inflammation-associated osteopenia. PloS one 9:e100669 [PubMed: 24971753]
3. Perryman L, Erler JT (2014) Lysyl oxidase in cancer research. Future Oncol 10:1709–1717 [PubMed: 25145437]
4. Kenyon K, Contente S, Trackman PC, Tang J, Kagan HM, Friedman RM (1991) Lysyl oxidase and rrg messenger RNA. Science 253:802 [PubMed: 1678898]
5. Liu G, Daneshgari F, Li M, Lin D, Lee U, Li T, Damaser MS (2007) Bladder and urethral function in pelvic organ prolapsed lysyl oxidase like-1 knockout mice. British Journal of Urology International 100:414–418
6. Panchenko MV, Stetler-Stevenson WG, Trubetskoy OV, Gacheru SN, Kagan HM (1996) Metalloproteinase activity secreted by fibrogenic cells in the processing of prolysyl oxidase. Potential role of procollagen C-proteinase. The Journal of biological chemistry 271:7113–7119 [PubMed: 8636146]
7. Trackman PC, Bedell-Hogan D, Tang J, Kagan HM (1992) Post-translational glycosylation and proteolytic processing of a lysyl oxidase precursor. The Journal of biological chemistry 267:8666–8671 [PubMed: 1349020]
8. Uzel MI, Scott IC, Babakhanlou-Chase H, Palamakumbura AH, Pappano WN, Hong HH, Greenspan DS, Trackman PC (2001) Multiple bone morphogenetic protein 1-related mammalian metalloproteinases process pro-lysyl oxidase at the correct physiological site and control lysyl oxidase activation in mouse embryo fibroblast cultures. The Journal of biological chemistry 276:22537–22543 [PubMed: 11313359]
9. Liu X, Zhao Y, Gao J, Pawlyk B, Starcher B, Spencer JA, Yanagisawa H, Zuo J, Li T (2004) Elastic fiber homeostasis requires lysyl oxidase-like 1 protein. Nature genetics 36:178–182 [PubMed: 14745449]
10. Wieslander CK, Rahn DD, McIntire DD, Acevedo JF, Drewes PG, Yanagisawa H, Word RA (2009) Quantification of pelvic organ prolapse in mice: vaginal protease activity precedes increased MOPQ scores in fibulin 5 knockout mice. Biology of reproduction 80:407–414 [PubMed: 18987327]
11. Kagan HM, Trackman PC (1991) Properties and function of lysyl oxidase. American journal of respiratory cell and molecular biology 5:206–210 [PubMed: 1680355]
12. Smith-Mungo LI, Kagan HM (1998) Lysyl oxidase: properties, regulation and multiple functions in biology. Matrix biology : journal of the International Society for Matrix Biology 16:387–398 [PubMed: 9524359]
13. Siegel RC (1979) Lysyl oxidase. International review of connective tissue research 8:73–118 [PubMed: 41816]
14. Kagan HM (1986) Characterization and Regulation of Lysyl Oxidase. In: Mecham RP (ed) Regulation of Matrix Accumulation. Academic Press, p 321–398
15. Hornstra IK, Birge S, Starcher B, Bailey AJ, Mecham RP, Shapiro SD (2003) Lysyl oxidase is required for vascular and diaphragmatic development in mice. The Journal of biological chemistry 278:14387–14393 [PubMed: 12473682]
16. Maki JM, Rasanen J, Tikkanen H, Sormunen R, Makikallio K, Kivirikko KI, Soininen R (2002) Inactivation of the lysyl oxidase gene Lox leads to aortic aneurysms, cardiovascular dysfunction, and perinatal death in mice. Circulation 106:2503–2509 [PubMed: 12417550]
17. Pischon N, Maki JM, Weisshaupt P, Heng N, Palamakumbura AH, N'Guessan P, Ding A, Radlanski R, Renz H, Bronckers TA, Myllyharju J, Kielbassa AM, Kleber BM, Bernimoulin JP, Trackman PC (2009) Lysyl oxidase (lox) gene deficiency affects osteoblastic phenotype. Calcified Tissue International 85:119–126 [PubMed: 19458888]
18. Simon LS (2007) Osteoporosis. Rheumatic Disease Clinics of North America 33:149–176 [PubMed: 17367698]

19. Shih MS, Cook MA, Spence CA, Palnitkar S, McElroy H, Parfitt AM Relationship between bone formation rate and osteoblast surface on different subdivisions of the endosteal envelope in aging & osteoporosis. Bone 14:519–521 [PubMed: 8363902]
20. Sanada H, Shikata J, Hamamoto H, Ueba Y, Yamamuro T, Takeda T (1978) Changes in collagen cross-linking and lysyl oxidase by estrogen. Biochimica et Biophysica Acta (BBA) - General Subjects 541:408–413 [PubMed: 27234]
21. Saito M, Marumo K (2010) Collagen cross-links as a determinant of bone quality: a possible explanation for bone fragility in aging, osteoporosis, and diabetes mellitus. Osteoporosis international : a journal established as result of cooperation between the European Foundation for Osteoporosis and the National Osteoporosis Foundation of the USA 21:195–214
22. Atsawasuwan P, Mochida Y, Parisuthiman D, Yamauchi M (2005) Expression of lysyl oxidase isoforms in MC3T3-E1 osteoblastic cells. Biochemical and biophysical research communications 327:1042–1046 [PubMed: 15652501]
23. Assaggaf MA, Kantarci A, Sume SS, Trackman PC (2015) Prevention of phenytoin-induced gingival overgrowth by lovastatin in mice. The American journal of pathology 185:1588–1599 [PubMed: 25843680]
24. Morgan EF, Mason ZD, Chien KB, Pfeiffer AJ, Barnes GL, Einhorn TA, Gerstenfeld LC (2009) Micro-computed tomography assessment of fracture healing: relationships among callus structure, composition, and mechanical function. Bone 44:335–344 [PubMed: 19013264]
25. Gere JM, Goodno BJ (2009) Mechanics of Materials. Cengage Learning. Inc.: Independence, KY
26. Buie HR, Campbell GM, Klinck RJ, MacNeil JA, Boyd SK (2007) Automatic segmentation of cortical and trabecular compartments based on a dual threshold technique for in vivo micro-CT bone analysis. Bone 41:505–515 [PubMed: 17693147]
27. Bouxsein ML, Boyd SK, Christiansen BA, Guldberg RE, Jepsen KJ, Muller R (2010) Guidelines for assessment of bone microstructure in rodents using micro-computed tomography. Journal of bone and mineral research : the official journal of the American Society for Bone and Mineral Research 25:1468–1486
28. Junqueira LC, Bignolas G, Brentani RR (1979) Picrosirius staining plus polarization microscopy, a specific method for collagen detection in tissue sections. Histochemical Journal 11:447–455
29. Vasikaran S, Eastell R, Bruyere O, Foldes AJ, Garnero P, Griesmacher A, McClung M, Morris HA, Silverman S, Trenti T, Wahl DA, Cooper C, Kanis JA (2011) Markers of bone turnover for the prediction of fracture risk and monitoring of osteoporosis treatment: a need for international reference standards. Osteoporosis international : a journal established as result of cooperation between the European Foundation for Osteoporosis and the National Osteoporosis Foundation of the USA 22:391–420
30. Iftikhar M, Hurtado P, Bais MV, Wigner N, Stephens DN, Gerstenfeld LC, Trackman PC (2011) Lysyl oxidase-like-2 (LOXL2) is a major isoform in chondrocytes and is critically required for differentiation. The Journal of biological chemistry 286:909–918 [PubMed: 21071451]
31. Martin A, Salvador F, Moreno-Bueno G, Floristan A, Ruiz-Herguido C, Cuevas EP, Morales S, Santos V, Csiszar K, Dubus P, Haigh JJ, Bigas A, Portillo F, Cano A (2015) Lysyl oxidase-like 2 represses Notch1 expression in the skin to promote squamous cell carcinoma progression. The EMBO journal 34:1090–1109 [PubMed: 25759215]
32. Tommasini SM, Morgan TG, van der Meulen M, Jepsen KJ (2005) Genetic variation in structure-function relationships for the inbred mouse lumbar vertebral body. Journal of bone and mineral research : the official journal of the American Society for Bone and Mineral Research 20:817–827
33. Lee UJ, Gustilo-Ashby AM, Daneshgari F, Kuang M, Vurbic D, Lin DL, Flask CA, Li T, Damaser MS (2008) Lower urogenital tract anatomical and functional phenotype in lysyl oxidase like-1 knockout mice resembles female pelvic floor dysfunction in humans. American journal of physiology. Renal physiology 295:F545–555 [PubMed: 18495804]
34. Kapczuk K, Sowinska-Przepiera E, Friebe Z (2003) [Osteoprotegerin/RANKL/RANK system and postmenopausal osteoporosis. The possible therapeutic aspects]. Ginekologia polska 74:323–331 [PubMed: 12916277]

35. Bouxsein ML, Myers KS, Shultz KL, Donahue LR, Rosen CJ, Beamer WG (2005) Ovariectomy-induced bone loss varies among inbred strains of mice. Journal of bone and mineral research : the official journal of the American Society for Bone and Mineral Research 20:1085–1092
36. Bord S, Ireland DC, Beavan SR, Compston JE (2003) The effects of estrogen on osteoprotegerin, RANKL, and estrogen receptor expression in human osteoblasts. Bone 32:136–141 [PubMed: 12633785]
37. Boyce BF, Xing L (2007) Biology of RANK, RANKL, and osteoprotegerin. Arthritis research & therapy 9 Suppl 1:S1 [PubMed: 17634140]
38. Bronson RE, Calaman SD, Traish AM, Kagan HM (1987) Stimulation of lysyl oxidase (EC 1.4.3.13) activity by testosterone and characterization of androgen receptors in cultured calf aorta smooth-muscle cells. The Biochemical journal 244:317–323 [PubMed: 2889450]
39. Ballanti P, Minisola S, Pacitti MT, Scarnecchia L, Rosso R, Mazzuoli GF, Bonucci E (1997) Tartrate-resistant acid phosphate activity as osteoclastic marker: sensitivity of cytochemical assessment and serum assay in comparison with standardized osteoclast histomorphometry. Osteoporosis international : a journal established as result of cooperation between the European Foundation for Osteoporosis and the National Osteoporosis Foundation of the USA 7:39–43
40. Biver E (2012) Use of bone turnover markers in clinical practice. Current Opinion in Endocrinology and Diabetes Obes 19:468–473
41. Garnero P, Ferreras M, Karsdal MA, Nicamhlaoibh R, Risteli J, Borel O, Qvist P, Delmas PD, Foged NT, Delaissé JM (2003) The Type I Collagen Fragments ICTP and CTX Reveal Distinct Enzymatic Pathways of Bone Collagen Degradation. Journal of Bone and Mineral Research 18:859–867 [PubMed: 12733725]
42. Koivula M-K, Risteli L, Risteli J (2012) Measurement of aminoterminal propeptide of type I procollagen (PINP) in serum. Clinical Biochemistry 45:920–927 [PubMed: 22480789]
43. Christiansen DL, Huang EK, Silver FH (2000) Assembly of type I collagen: fusion of fibril subunits and the influence of fibril diameter on mechanical properties. Matrix Biology 19:409–420 [PubMed: 10980417]
44. Muiznieks LD, Keeley FW (2013) Molecular assembly and mechanical properties of the extracellular matrix: A fibrous protein perspective. Biochimica et Biophysica Acta (BBA) - Molecular Basis of Disease 1832:866–875 [PubMed: 23220448]
45. Ottani V, Raspanti M, Ruggeri A (2001) Collagen structure and functional implications. Micron 32:251–260 [PubMed: 11006505]
46. Gualeni B, Rajpar MH, Kellogg A, Bell PA, Arvan P, Boot-Handford RP, Briggs MD (2013) A novel transgenic mouse model of growth plate dysplasia reveals that decreased chondrocyte proliferation due to chronic ER stress is a key factor in reduced bone growth. Disease Models and Mechechanisms 6:1414–1425
47. Wang G, Woods A, Agoston H, Ulici V, Glogauer M, Beier F (2007) Genetic ablation of Rac1 in cartilage results in chondrodysplasia. Developmental biolology 306:612–623
48. Lucero HA, Ravid K, Grimsby JL, Rich CB, DiCamillo SJ, Maki JM, Myllyharju J, Kagan HM (2008) Lysyl oxidase oxidizes cell membrane proteins and enhances the chemotactic response of vascular smooth muscle cells. The Journal of biological chemistry 283:24103–24117 [PubMed: 18586678]
49. Atsawasuwan P, Mochida Y, Katafuchi M, Kaku M, Fong KS, Csiszar K, Yamauchi M (2008) Lysyl oxidase binds transforming growth factor-beta and regulates its signaling via amine oxidase activity. The Journal of biological chemistry 283:34229–34240 [PubMed: 18835815]
50. Li W, Nugent MA, Zhao Y, Chau AN, Li SJ, Chou IN, Liu G, Kagan HM (2003) Lysyl oxidase oxidizes basic fibroblast growth factor and inactivates its mitogenic potential. Journal of cellular biochemistry 88:152–164 [PubMed: 12461785]
51. Le Provost GS, Debret R, Cenizo V, Aimond G, Pez F, Kaniewski B, Andre V, Sommer P (2010) Lysyl oxidase silencing impairs keratinocyte differentiation in a reconstructed-epidermis model. Experimental dermatology 19:1080–1087 [PubMed: 20812961]
52. Palamakumbura AH, Vora SR, Nugent MA, Kirsch KH, Sonenshein GE, Trackman PC (2009) Lysyl oxidase propeptide inhibits prostate cancer cell growth by mechanisms that target FGF-2-cell binding and signaling. Oncogene 28:3390–3400 [PubMed: 19597471]

53. Kirschmann DA, Seftor EA, Fong SF, Nieva DR, Sullivan CM, Edwards EM, Sommer P, Csiszar K, Hendrix MJ (2002) A molecular role for lysyl oxidase in breast cancer invasion. Cancer research 62:4478–4483 [PubMed: 12154058]

54. Li J, Gu X, Ma Y, Calicchio ML, Kong D, Teng YD, Yu L, Crain AM, Vartanian TK, Pasqualini R, Arap W, Libermann TA, Snyder EY, Sidman RL (2010) Nna1 mediates Purkinje cell dendritic development via lysyl oxidase propeptide and NF-kappaB signaling. Neuron 68:45–60 [PubMed: 20920790]

55. Vora SR, Palamakumbura AH, Mitsi M, Guo Y, Pischon N, Nugent MA, Trackman PC (2010) Lysyl oxidase propeptide inhibits FGF-2-induced signaling and proliferation of osteoblasts. The Journal of biological chemistry 285:7384–7393 [PubMed: 20048148]

56. Uveges TE, Collin-Osdoby P, Cabral WA, Ledgard F, Goldberg L, Bergwitz C, Forlino A, Osdoby P, Gronowicz GA, Marini JC (2008) Cellular Mechanism of Decreased Bone in Brtl Mouse Model of OI: Imbalance of Decreased Osteoblast Function and Increased Osteoclasts and Their Precursors. Journal of Bone and Mineral Research 23:1983–1994 [PubMed: 18684089]

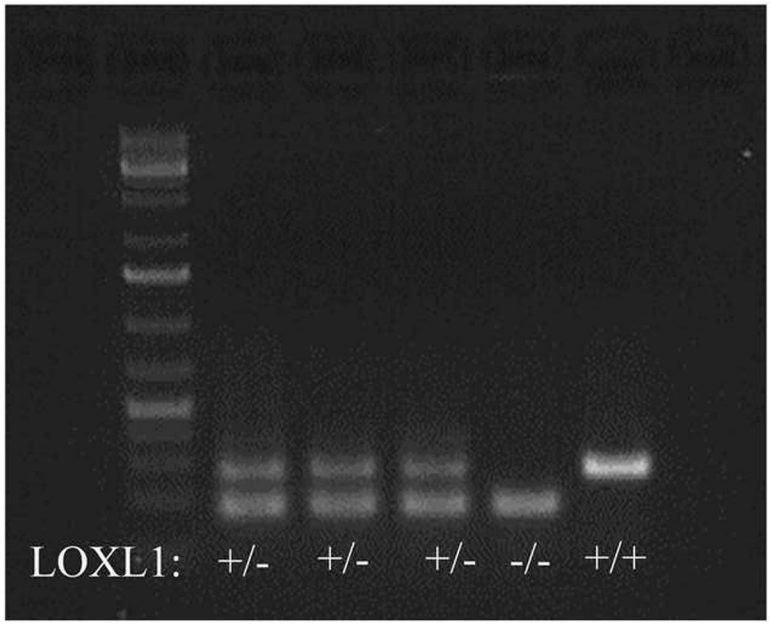

Figure 1. Absence of LOXL1 in femur tissue from *Loxl1* −/− mice.

Genotyping of mouse tail tip DNA shows the presence of a single 175 bp band corresponding to the mutant gene and the absence of the larger band corresponding to the wild type *LOXL1* gene. Genotype designations are under each lane. The marker is a 1 Kbp ladder.

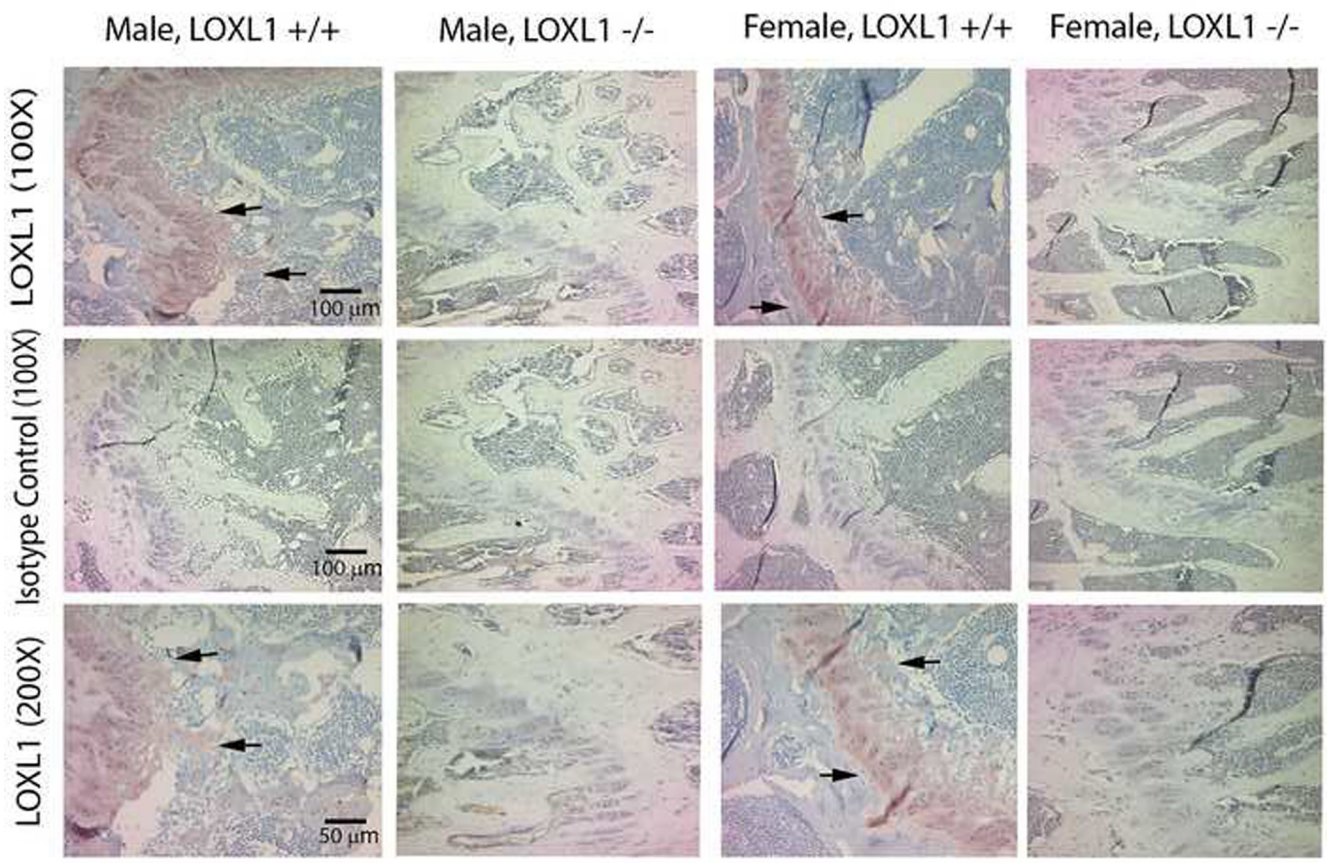

Figure 2. Absence of LOXL1 in *LOXL1−/−* bones.

LOXL1 antibody (Abbiotec #252215) or IgG isotype control were employed to stain femurs from *LOXL1−/−* mice and wild type littermates. Arrows mark the growth plates which contain high in LOXL1 staining in wild type mice. *LOXL1−/−* femurs contain no LOXL1 staining. Scale bars, 100 μm for 100X magnification and 50 μm for 200X magnification.

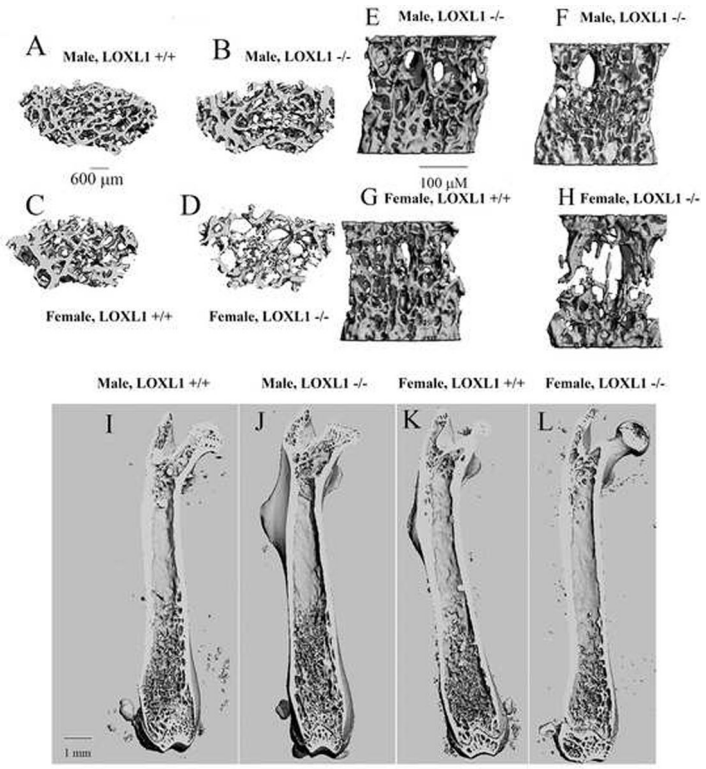

Figure 3. Micro-computed tomography of *Loxl1*−/− and wild type mouse bones.

Three-dimensional images (transverse view) for the femoral distal metaphysis (A-D) representing wild type and *LOXL1* −/− male and female mice. Images are representative of eight animals analyzed. (E-H) Images for L5 vertebrae (sagittal view) representing wild-type and *LOXL1* −/− male and female mice. Images are representative of eight animals analyzed per group. (I-L) Representative full-length, cross-sectional views of the femur from wild type and *LOXL1* −/− male and female mice showing the same overall length of femurs, but trabecular deficiencies in female *LOXL1*−/− femurs.

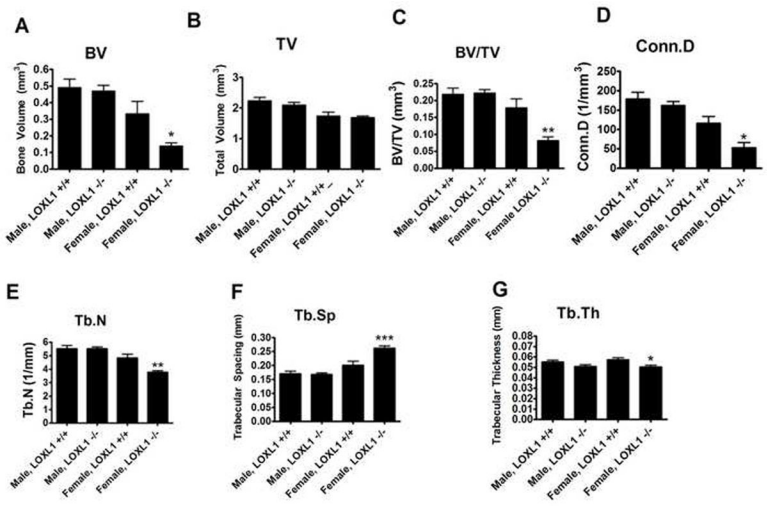

Figure 4. Trabecular bone parameters from femur distal metaphysis from wild type and *LOXL1*−/− male and female mice.

Data are (mean values +/− SD). One asterisk (*) indicates significant difference from wild-type mice of the same sex with p<.01, two asterisks (**) indicate p<.001, and three asterisks indicate p<.0001 by one-way ANOVA and Tukey's multiple comparison test; n=8

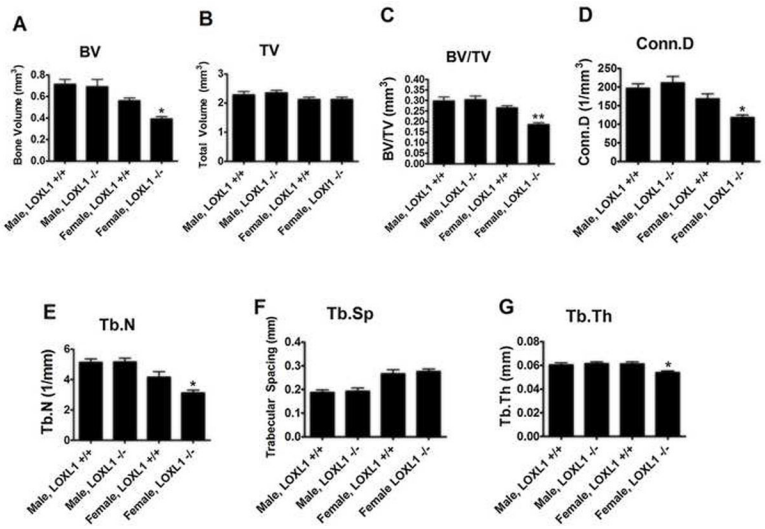

Figure 5. Trabecular bone parameters from L5 vertebrae representing wild type and *LOXL1*−/− male and female mice.

Data are (mean values +/− SD). One asterisk (*) indicates significant difference from wild-type mice of the same sex with p<.01, two asterisks (**) indicate p<.001, and three asterisks indicate p<.0001 by one-way ANOVA and Tukey's multiple comparison test; n=8

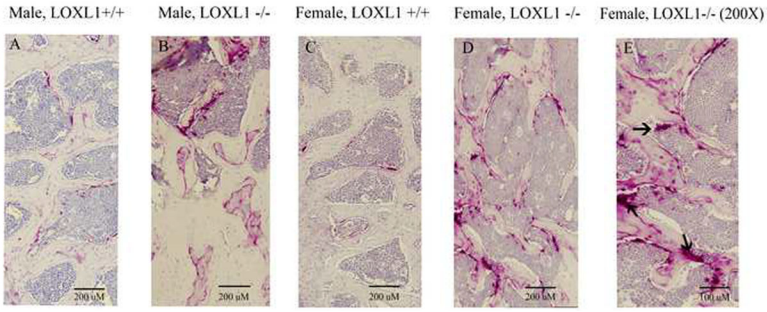

Figure 6. TRAP staining of representative sagittal sections of femurs.

(A-D) Images are from the area directly proximal to the distal growth plates representing wild type and *LOXL1−/−* male and female mice; scale bar, 200 uM. **(E)** Panel D at higher magnification (200X). Arrows indicate TRAP positive osteoclasts. Scale bar, 100 μM.

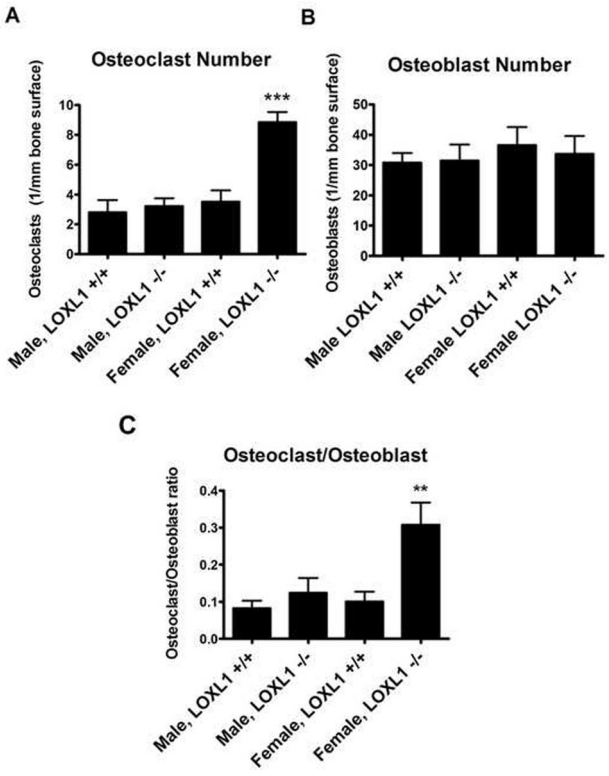

Figure 7. (A) Histomorphometric analyses of histological sections of femur sections analyzed for number of TRAP positive osteoclasts in wild type and *LOXL1*−/− male and female mice.

Data are (mean values +/− SD). One asterisk (*) indicates significant difference from wild-type mice of the same sex with p<.01, two asterisks (**) indicate p<.001, and three asterisks indicate p<.0001 by one-way ANOVA and Tukey's multiple comparison test; n=8. (B) Histomorphometric analyses of histological sections of femur sections analyzed for number of osteoblasts. Asterisk notation is the same, n=8 (C) Calculated ratio of osteoclasts to osteoblasts. Asterisk notation is the same, n=8.

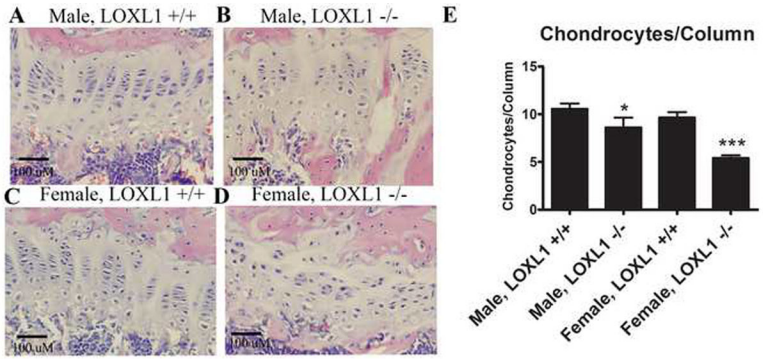

Figure 8. Hematoxylin and eosin staining of representative sagittal sections of femur distal growth plates.

(A) Images are from wild type and *LOXL1−/−* male and female mice; scale bar, 100 μM.

(B) Histomorphometric analyses of histological sections of femur sections for chondrocytes per column of wild type and mutant male and female mice. Asterisk notation is the same as in Figure 6, n=8.

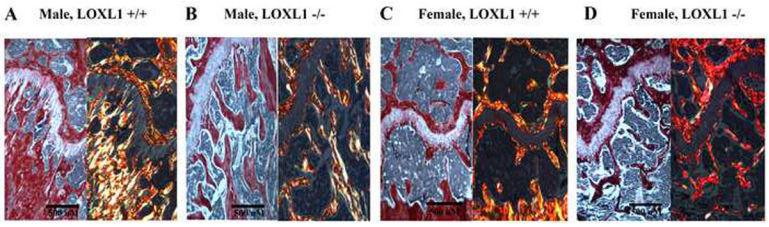

Figure 9. Picrosirius red staining of representative sagital sections of femurs.

Images are from the area starting at the center of the growth plate extending ~2mm to the right from wild type and *LOXL1*−/− male and female mice. Scale bar, 500 μM.

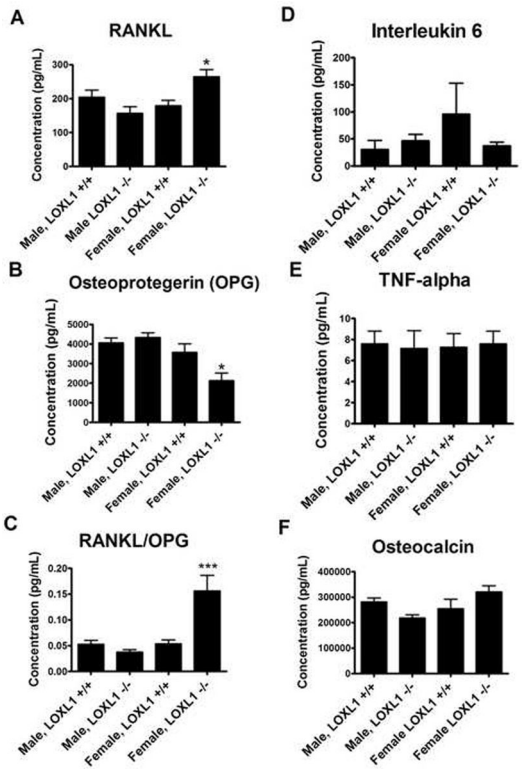

Figure 10. Concentration (pg/mL) of OPG, RANKL, Interleukin 6, TNF-α, and osteocalcin in the serum of wild type and *LOXL1*−/− male and female mice.

Data are mean values in pg/ml +/− SD. One asterisk (*) indicates significant difference from wild-type mice of the same sex with p<.01, two asterisks (**) indicate p<.001, and three asterisks indicate p<.0001 by one-way ANOVA and Tukey's multiple comparison test; n=8.

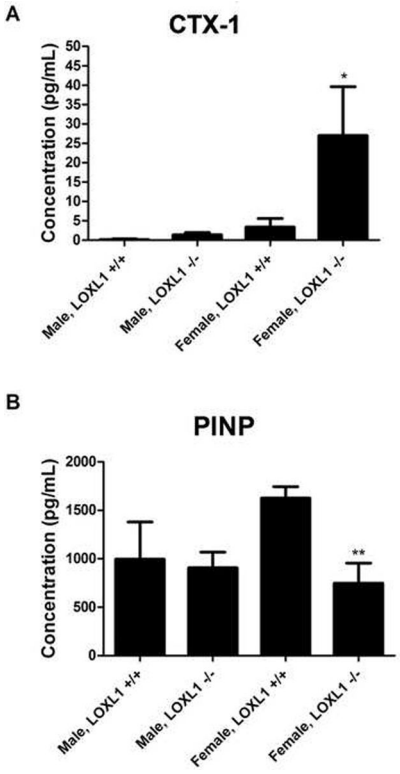

Figure 11. Concentration (pg/mL) of PINP and CTX-1 in the serum of wild type and *LOXL1*−/− male and female mice.

Data are mean values in pg/ml +/− SD. One asterisk (*) indicates significant difference from wild-type mice of the same sex with p<.05 and two asterisks (**) indicate p<.01 by one-way ANOVA and Tukey's multiple comparison test; n=6.

Table 1

Left Femur Lengths in and Weights of Wild Type and *Loxl1* −/− Mice

Genotype	Sex	Mean Femur Length (mm) +/− SD	Mean Weight (grams) +/− SD	N
Wild type	Male	16.03 +/− 0.32	37.7 +/− 4.3	8
Wild type	Female	15.95 +/− 0.65	26.05 +/− 4.7	8
Loxl1 −/−	Male	16.23 +/− 0.17	36.21 +/− 3.14	8
Loxl1 −/−	Female	16.03 +/− 0.48	26.1 +/− 3.19	8

Table 2

Bone Volume/Total Volume (BV/TV) of Cortical Bone

	Male, LOXL1 +/+	Male, LOXL1 −/−	Female, LOXL1 +/+	Female, LOXL1 −/−
Femur	0.543 +/− .02	0.529 +/− .03	0.512 +/− .03	0.487 +/− .03
Vertebrae	0.598 +/− .13	0.639 +/− .03	0.629 +/− .05	0.638 +/− .06